Charge ordering and phase competition in the layered perovskite $LaSr_2Mn_2O_7$

D. N. Argyriou* and H. N. Bordallo†
Los Alamos Neutron Science Center, Los Alamos National Laboratory, Los Alamos, New Mexico 87545

B. J. Campbell* and A. K. Cheetham
Materials Research Laboratory, University of California, Santa Barbara, California 93106

D. E. Cox
Department of Physics, Brookhaven National Laboratory, Upton, New York 11973

J. S. Gardner‡
MST-10, Los Alamos National Laboratory, Los Alamos, New Mexico 80434

K. Hanif
Department of Chemistry, University of California, Santa Barbara, California 93106

A. dos Santos
Materials Research Laboratory, University of California, Santa Barbara, California 93106

G. F. Strouse
Department of Chemistry, University of California, Santa Barbara, California 93106
(Received 13 December 1999)

Charge-lattice fluctuations are observed in the layered perovskite manganite $LaSr_2Mn_2O_7$ by Raman spectroscopy at temperatures as high as 340 K, and with decreasing temperature they become static, forming a charge-ordered (CO) phase below $T_{CO}=210$ K. In the static regime, superlattice reflections are observed by neutron and x-ray diffraction with a propagation vector (1/4, −1/4, 0). Crystallographic analysis of the CO state demonstrates that the degree of charge and orbital ordering in this manganite is weaker than that in the three-dimensional perovskite manganites. Below $T_N=170$ K, type-*A* antiferromagnetism (AF) develops and competes with the charge ordering, causing it to eventually melt below $T^*=100$ K. High-resolution diffraction measurements suggest that the CO and AF states do not coincide within the same region of material, but rather coexist as separate phases. The transition to type-*A* antiferromagnetism at lower temperatures is characterized by the competition between these two phases.

I. INTRODUCTION

The competition between charge, lattice, and spin degrees of freedom can be delicately balanced to form materials where electrons localize on alternate transition metal sites on a lattice. So-called *charge-ordered* (CO) lattices have been observed for a number of transition-metal perovskites and are fundamental in the understanding of the physical properties of many of these materials. For example, the formation of dynamic charge ordering fluctuations has recently been reported in superconducting $La_{1.85}Sr_{0.15}CuO_4$ (Ref. 1) and $YBa_2Cu_3O_{7-x}$,[2] while in $Pr_{0.7}Ca_{0.3}MnO_3$, a ferromagnetic metallic phase forms from the melting of a charged-ordered lattice when irradiated with x-rays.[3] The fundamental physics governing these phenomena is applicable to a wide range of materials including linear chain systems, conducting organic materials, and magnetic semiconductors.[4,5]

The observation of colossal negative magnetoresistance (CMR) in the layered manganites $La_{2-2x}Sr_{1+2x}Mn_2O_7$ (Ref. 6) has provided the opportunity to study the strong interplay among charge, spin, and lattice degrees of freedom in reduced dimensions, and also to explore novel phenomena that are not found in the three-dimensional (3D) perovskite manganites. For example, the natural stacking of $(La,Sr)MnO_3$ perovskite bilayers separated by (La, Sr)O blocking layers forms the framework of tunneling structures and spin valves in a single chemical phase, as opposed to the larger scale heterostructures obtained by thin-film deposition.[7,8]

Recently, CO has been reported in layered $LaSr_2Mn_2O_7$ ($x=0.5$). However, unlike the 3D perovskite compounds, the CO state is stable only over a limited temperature range (~100–200 K).[9] This suggests that the lower dimensionality of this material directly effects the competition between charge, lattice, and spin degrees of freedom. Charge and orbital ordering in the manganite perovskites bring into focus the overall issue of the influence of electron-phonon coupling on the transport and magnetic properties of these materials.

In this paper we report neutron, x-ray, and resonant Raman scattering measurements on $LaSr_2Mn_2O_7$. We find that charge-lattice fluctuations arising from perturbations in the local crystal structure from hopping e_g carriers are evident in resonant Raman measurements as high as 340 K. With decreasing temperature these fluctuations become static below $T_{CO}=210$ K and superlattice reflections indicative of charge ordering are observed using both neutron and x-ray diffraction. Analysis of single-crystal neutron diffraction data

shows that the structure of $LaSr_2Mn_2O_7$ is characterized by partial charge localization, as measured from the degree of structural distortion around nominally Mn^{3+} and Mn^{4+} sites. With decreasing temperature the development of the CO phase is disrupted by the onset of a type-*A* antiferromagnetic (AF) ordering of Mn spins at $T_N = 170$ K. As the CO lattice melts and disappears below $T^* = 100$ K, charge-lattice fluctuations reappear and remain at low temperatures. The competition between the charge-ordered and type-*A* AF phase is highlighted by the broadening and eventual splitting of diffraction profiles. This behavior suggests that charge ordering and antiferromagnetism do not coincide in these materials, but rather coexist as separate phases. At low temperature we find evidence for only a type-*A* antiferromagnetic insulating phase.

II. EXPERIMENT

Neutron diffraction data from a single crystal of $LaSr_2Mn_2O_7$ ($x = 0.5$) were measured as a function of temperature (300–20 K) using the single-crystal diffractometer (SCD) at the Los Alamos Neutron Science Center, Los Alamos National Laboratory. The crystal was cleaved from a boule prepared by the optical floating-zone method. Single crystals from this boule have also been characterized with resistivity and inductively coupled plasma (ICP) spectroscopy measurements. The resistivity measurements in the *ab* plane showed a broad peak between 210 and 150 K associated with charge ordering [see Fig. 1(a)] and are in agreement with the measurements of Kimura *et al.*[9] ICP measurements gave a composition of $x = 0.50(2)$ for the single-crystal sample.

A powder sample of $LaSr_2Mn_2O_7$ was also prepared from sol-gel precursors. Stoichiometric amounts of $La(OH)_3$, MnO, and $SrCO_3$ were dissolved in glacial acetic acid and stirred for several hours at about 80 °C. After boiling off all the acid, the resulting pink gel was dried at 400 °C for 4 h, annealed at 1400 °C for 24 h, and quenched to room temperature, all in air. The powder sample was characterized by x-ray powder diffraction measured from 300 to 20 K on the high-resolution powder diffractometer X7A at the National Synchrotron Light Source, Brookhaven National Laboratory. For this experiment the sample was mounted in a 0.4 mm glass capillary, and data were collected using a wavelength of 0.8 Å and a Ge(111)/Ge(220) monochromator-analyzer combination. From the linewidths of the x-ray diffraction data, we estimated the compositional fluctuations to be ± 0.02 [i.e., $x = 0.50(2)$].

The powder sample was also used in measuring resonant Raman scattering as a function of temperature (16–340 K) using laser wavelengths of 2.41, 2.54, and 2.7 eV. Measurements were made in a backscattering configuration using an Ar^+-ion laser excitation (3 mW incident power) coupled to a Notch filter 0.5 M ARC single spectrograph (1800 lines mm-1/400 blaze), and a Princeton Instrument 512×512 charge-coupled diode (CCD) array for detection. Temperature control at ± 1.0 K was provided by an APD closed-cycle He cryostat controlled by a SI9620-1 temperature controller. Our data confirmed that power densities over 5 mW result in irreversible photodamage to the manganite sample as observed previously in $LaMnO_3$ by Iliev *et al.*[10]

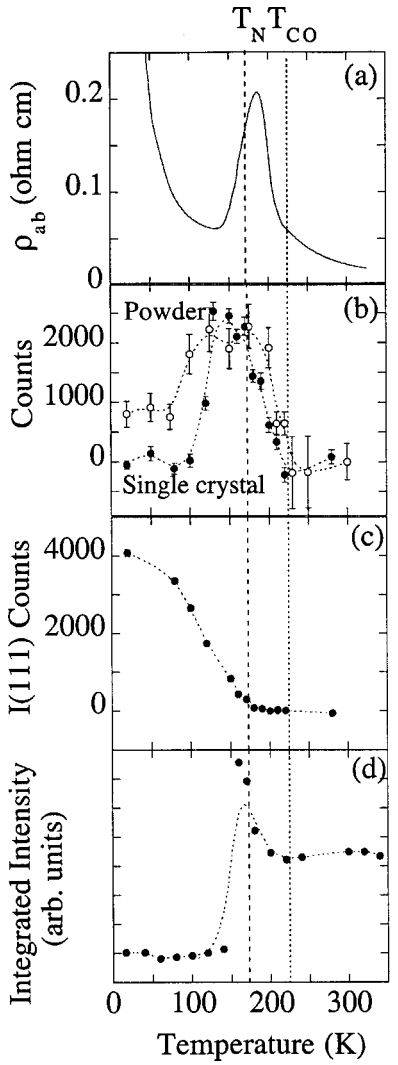

FIG. 1. (a) In-plane resistivity as a function of temperature from a $LaSr_2Mn_2O_7$ single crystal. (b) Temperature dependence of the (1.75,2.25,0) superlattice reflection measured from the single-crystal sample using neutron diffraction (solid symbols) and the (0.25,1.75,0) superlattice reflection measured from the powder sample using x-ray diffraction (open symbols). (c) Temperature dependence of the (111) type-*A* antiferromagnetic reflection measured from the single-crystal sample using neutron diffraction. (d) Temperature dependence of the intensity of the in-plane Mn-O(3) bond bending mode (δ_3) and the coupled resonant mode (δ_3'). Each point represents an integration of the observed spectra from 440 to 545 cm^{-1}. The dashed line through the data is a guide to the eye.

III. CHARGE ORDERING AND PHASE COEXISTENCE IN $LaSr_2Mn_2O_7$

Room-temperature neutron and x-ray diffraction measurements for both single-crystal and powder samples were consistent with the well-known $I4/mmm$ crystal structure.[11] On cooling these samples below $T_{CO} = 210$ K, weak superlattice reflections with a propagation vector $\mathbf{q} = (1/4,1/4,0)$ were observed, in agreement with measurements reported by Kimura *et al.*[9] The intensities of the superlattice reflections approximately track the in-plane resistivity, reaching a maximum at ~150 K with decreasing temperature and disappearing below $T^* = 100$ K in our single-crystal neutron measurements [see Fig. 1(b)].[9] This is in sharp contrast to the perov-

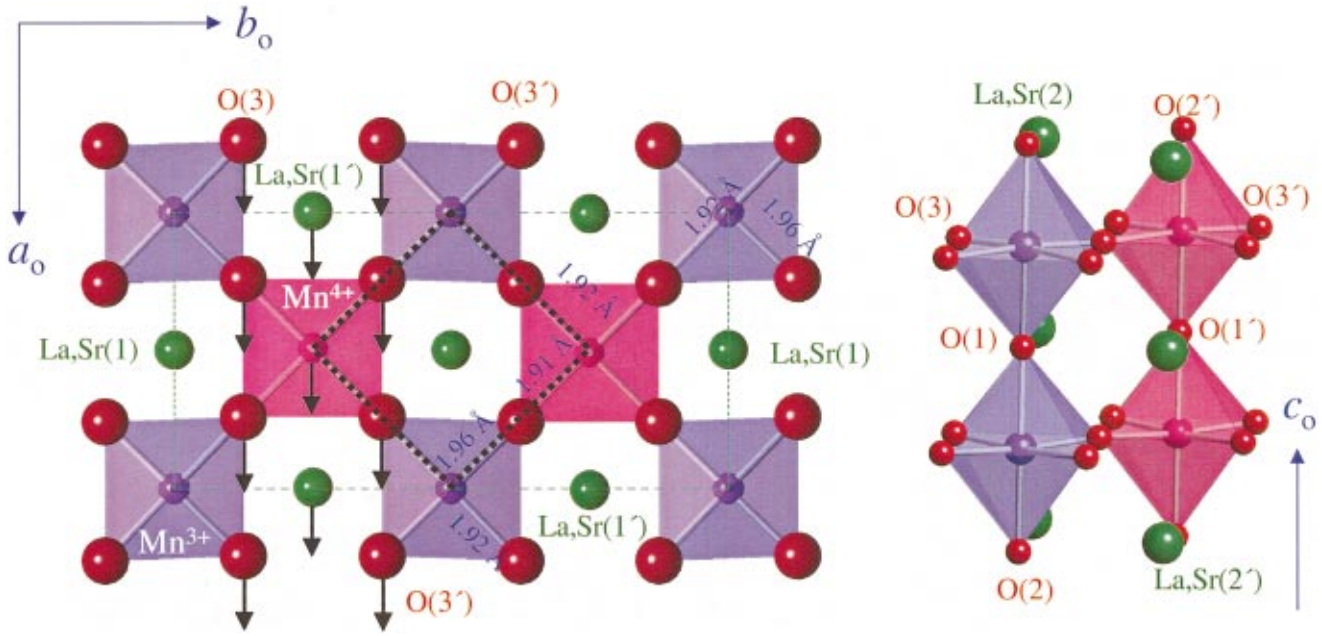

FIG. 2. (Color) The crystal structure of the CO state of $LaSr_2Mn_2O_7$. The black thick lines show the cell of the parent $I4/mmm$ structure, while the thinner green lines shows the size of the $\sqrt{2}a_t \times 2\sqrt{2}a_t \times c_t$ supercell. Arrows show the displacement of atoms from the parent $I4/mmm$ structure. Atoms labeled as $(\prime)$ indicate equivalent sites in the $I4/mmm$ setting. Various Mn-O bond lengths are shown.

skite $La_{1/2}Ca_{1/2}MnO_3$ where the CO state is stable to at least 5 K.[12] We observe a similar decrease in intensity at ~90 K in the powder sample [Fig. 1(b)], but the superlattice reflections do not disappear completely and are still visible at 20 K. We attribute this to extrinsic effects such as pinning by grain boundaries or point defects. We also note that the widths of the superlattice reflections in both the single-crystal and powder samples remain close to the instrumental resolution over the temperature ranges in which they are observed, suggesting coherence lengths of hundreds to thousands of angstroms. In addition to these superlattice reflections, magnetic reflections are observed below $T_N = 170$ K in our single-crystal measurements, consistent with a type-*A* AF phase [Fig. 1(c)].

A detailed crystallographic description of the charge and orbital ordering in $LaSr_2Mn_2O_7$ is obtained by analyzing the single-crystal neutron diffraction data measured at 160 K. The additional superlattice reflections can be indexed on a commensurate orthorhombic supercell of $a_0 \sim \sqrt{2}a_t$, $b_0 \sim 2\sqrt{2}a_t$, $c_0 = c_t$ (where a_t and c_t are the parent tetragonal lattice constants) as shown in Fig. 2. The observation of these superlattice reflections by neutrons and x rays clearly suggests that they arise from structural changes as opposed to the magnetic ordering as suggested by Kubota *et al.*[13] In addition, recent polarized neutron measurements from the same single-crystal sample used in this work clearly show that the superlattice reflections reported here exhibit no significant magnetic component.[14] The observed extinction conditions for the superstructure reflections are consistent with space group *Bbmm*. This reduced symmetry provides for two different Mn sites [Mn(1) and Mn(1′)], where the surrounding in-plane oxygens can relax in both the a_0 and b_0 directions (see Fig. 2) compared to the parent $I4/mmm$ structure. We note here that between T_{CO} and T^* only an *average* structure description of $LaSr_2Mn_2O_7$ can be obtained using the parent space group symmetry $I4/mmm$. The details of the charge ordered structure are entirely contained in the weaker superlattice reflections.

During the analysis of the single-crystal data, we found that displacements from the average structure along the b_0 and c directions did not compute significant intensity for superlattice reflections, while displacements along a_0 did. In the final model, only displacements along a_0 were refined for the Mn(1′) site (labeled at Mn^{4+} in Fig. 2), its surrounding oxygen atoms [O(3), O(3′), O(1′), and O(2′)] and the La and Sr atoms above and below the Mn(1′) site [La, Sr(1′) and La, Sr(2′)]. The superstructure was refined using only superlattice reflections as their low intensities (~0.7% of the parent Bragg reflection) do not contribute significantly to the overall χ^2 of the refinement when all observed reflections are considered. The final refinement produced a weighted *R* factor $wR(F^2)$ of 20.1% for the refinement using superlattice reflections only and 7.75% for all reflections. Refined crystallographic parameters for the charge-ordered structure of $LaSr_2Mn_2O_7$ are given in Table I.

Two distinct Mn sites are identified from the analysis of the single-crystal neutron diffraction data (see Fig. 2), consistent with a structural distortion arising from the localization and ordering of e_g carriers. The Mn(1) site exhibits two short in-plane Mn-O bonds of 1.923(1) Å and two long bonds of 1.962(1) Å, the latter corresponding to occupied $d_{3z^2-r^2}$ orbitals extended along the bond axis. The second site, Mn(1′), has two similar pairs of in-plane Mn-O bonds of 1.918(1) Å and 1.906(1) Å (see Fig. 2). The apical oxygen distances for both Mn sites are 1.921(2) Å for the Mn-O(1) and 1.944(2) Å for the Mn-O(2) bond. Differences in electron density between the two Mn sites are evident in the bond valence sums ν_{ij}, where we obtain values of 3.67 and 3.87 for the Mn(1) and Mn(1′) sites, respectively. These values suggest that the ionic model of CO in $LaSr_2Mn_2O_7$, in which discreet Mn^{3+} and Mn^{4+} sites exist due to the localization of e_g carriers, is oversimplified and a large degree of

TABLE I. Crystallographic parameters for the CO state of $LaSr_2Mn_2O_7$ at 160 K as measured using single-crystal neutron diffraction measurements. For the average structure refinements, 900 reflections were used and a $wR(F^2)$ of 7.8% was obtained. For the superstructure refinements, 1901 superstructure reflections were measured, 1046 of which have $I>0$ and 68 have $I>3\sigma$. The lattice constants were found to be $a=5.443(4)$ Å, $b=10.194(4)$ Å, $c=19.816(15)$ Å. The y coordinates were not refined. Temperature factors were constrained as follows: $U(\mathrm{Mn}(1))=U(\mathrm{Mn}(1'))$, $U(\mathrm{La,Sr}(1))=U(\mathrm{La,Sr}(1'))=U(\mathrm{La,Sr}(2))=U(\mathrm{La,Sr}(2'))$, and for the oxygen atoms $U(\mathrm{O}(1))=U(\mathrm{O}(1'))$, $U(\mathrm{O}(2))=U(\mathrm{O}(2'))$, $U(\mathrm{O}(3))=U(\mathrm{O}(3'))$. Various Mn-O bond lengths computed from the structural parameters are also given below.

	x	y	z	U_{ISO} (Å^2)
$Mn^{3+}(1)$	0	0	0.09696(4)	0.0021(1)
$Mn^{4+}(1')$	0.5065(2)	0.25	0.09696(4)	0.0021(1)
La,Sr(1)	0	0	0.5	0.0051 (1)
La,Sr(1′)	0.5218(5)	0.25	0.5	0.0051(1)
La,Sr(2)	0	0	0.31788(2)	0.0051(1)
La,Sr(2′)	0.5073(5)	0.25	0.31788(2)	0.0051(1)
O(1)	0	0	0	0.0098(2)
O(1′)	0.5164(7)	0.25	0	0.0098(2)
O(2)	0	0	0.19505(3)	0.0099(4)
O(2′)	0.5035(4)	0.25	0.19505(3)	0.0099(4)
O(3)	0.2588(2)	0.125	0.09495(2)	0.0077(1)
O(3′)	0.7510(2)	0.125	0.09495(2)	0.0077(1)

$Mn^{3+}(1)$-O(3′)	1.962(1) Å	$Mn^{4+}(1)$-O(3′)	1.906(1) Å
$Mn^{3+}(1)$-O(3)	1.923(1) Å	$Mn^{4+}(1)$-O(3)	1.918(1) Å
$Mn^{3+}(1)$-O(1)	1.921(2) Å	$Mn^{4+}(1)$-O(1′)	1.921(2) Å
$Mn^{3+}(1)$-O(2)	1.944(2) Å	$Mn^{4+}(1)$-O(2′)	1.944(2) Å

covalency involving Mn d orbitals and O p orbitals may exist.

The structural model of the charge-ordered state in $LaSr_2Mn_2O_7$ presented here is essentially the same as that proposed by Goodenough[15] and recently observed by Radaelli *et al.*[12] for the manganite perovskite $La_{1/2}Ca_{1/2}MnO_3$. However, a clear difference exists in the bond valences of the Mn sites. For $La_{1/2}Ca_{1/2}MnO_3$, the nominally Mn^{4+} and Mn^{3+} sites have bond valance values of 3.9 and 3.5, respectively,[12] suggesting that the degree of charge ordering in $LaSr_2Mn_2O_7$ is smaller than that observed in the perovskite manganites. In addition, the partial *charge* ordering is also reflected in a partial *orbital* ordering; charge is shared unequally between $d_{x^2-y^2}$ and $d_{3z^2-r^2}$ orbitals. Typically, filled Mn^{3+} $d_{3z^2-r^2}$ orbitals produce a bond length of ~2.1 Å, larger than the value of 1.962 Å observed for $LaSr_2Mn_2O_7$, while empty $d_{x^2-y^2}$ orbitals have a bond length of 1.91 Å, smaller than the 1.923 Å observed in $LaSr_2Mn_2O_7$.[16] These values suggest that the former orbital is underoccupied, while the latter is not completely empty.

As described by Goodenough[15] in the 1950s, the ordering of Mn $d_{3z^2-r^2}$ orbitals in $La_{1/2}Ca_{1/2}MnO_3$ gives rises to staggered *ferromagnetic* interactions between filled Mn^{3+} and empty Mn^{4+} d orbitals and *antiferromagnetic* interactions between empty Mn^{3+} and Mn^{4+} d orbitals. The arrangement of Mn spins that arises from these interactions is known as the CE magnetic structure. That the orbital ordering observed

TABLE II. Crystal and magnetic structure parameters for $LaSr_2Mn_2O_7$ at 20 K determined using single-crystal neutron diffraction. At 20 K no superlattice reflections were observed. The crystal structure was analyzed using the tetragonal $I4/mmm$ crystal structure (Ref. 11). The magnetic structure was analyzed in term of a type-A Mn spin arrangement; Mn spins lie ferromagnetically within MnO_2 along the ab plane, while the coupling between sheets is antiferromagnetic (Ref. 17). In all, 624 reflections were measured. Least-squares refinement of the model produced a $wR(F^2)$ of 9%. The lattice constants were found to be $a=3.852(3)$ Å, $c=19.76(2)$ Å. Various Mn-O bond lengths computed from the structural parameters are also given below.

	x	y	z	U_{ISO} (Å^2)
$Mn^{3+}(1)$	0	0	0.09701(16)	0.005(3)
$\mu_{ab}=2.63(6)$				
La,Sr(1)	0	0	0.5	0.0012(4)
La,Sr(2)	0	0	0.31819(8)	0.0024(3)
O(1)	0	0	0	0.0064(6)
O(2)	0	0	0.19516(13)	0.0065(5)
O(2′)	0.5	0	0.09490(9)	0.0047(3)

Mn(1)-O(1)	1.916(4) Å
Mn(1)-O(2)	1.939(5) Å
Mn(1)-O(3)	1.9291(13) Å

in $LaSr_2Mn_2O_7$ and $La_{1/2}Ca_{1/2}MnO_3$ is essentially identical would suggest that a similar magnetic ordering would be observed in both compounds. Surprisingly, our low-temperature neutron diffraction measurements show new magnetic reflections indicative of a type-A antiferromagnetic ordering[17] as well as nuclear reflections consistent with the well-known $I4/mmm$ crystal structure.[11] In the type-A antiferromagnetic structure, Mn moments form ferromagnetic MnO_2 sheets that are antiferromagneticaly coupled along the c axis and within and between perovskite bilayers (see Table II for crystal and magnetic parameters determined at 20 K). The observation of CE-type orbital ordering and type-A antiferromagnetism is contrary to Goodenough's rules for ferromagnetic and antiferromagnetic Mn^{3+}-O-Mn^{4+} coupling. This suggests that in the case of weak charge and orbital ordering, the application of Goodenough's rules to predict magnetic structure may not be entirely appropriate.

The resolution of this apparent contradiction between the observation of CE-type charge and orbital ordering and type-A antiferromagnetic ordering lies in the competition of between the CO and AF phases. Below T_{CO}, the resistivity increases as the charge-lattice fluctuations become static (see below). However, the decrease in resistivity and in the intensity of the superlattice reflections with decreasing temperature coincides with the onset of antiferromagnetism. Interestingly, the temperature dependence of the peak width of the (0 0 10) Bragg reflection provides insight into the competition between these two phases. It is common to use the (0 0 10) reflection to probe the homogeneity of a layered manganite sample, as it is a good indicator of the distribution of c-axis lattice parameters and is free of overlap from nearby reflections.[7,17] Using high-resolution synchrotron x-ray diffraction, we find that the (0 0 10) reflection at high temperatures is symmetrical, the only significant change be-

ing the continuous shift towards higher 2θ as the *c*-axis lattice parameter contracts with decreasing temperature (Fig. 4). Below T_N a high-angle shoulder develops, marking the formation of a new phase with a slightly lower value of the *c*-axis lattice parameter. The loss of intensity from the original peak makes it clear that the new magnetically ordered phase is forming at the expense of the CO phase formed at a higher temperature. By 125 K there are nearly equal amounts of the two phases, and by 50 K the new phase has almost entirely consumed the first. This suggests that the type-*A* AF phase and the CO phase do not coincide in the material, but rather coexist as separate and distinct phases. We note that this phase coexistence separates the magnetic and charge-lattice degrees of freedom in the system and thus lifts the apparent contradiction between CE-type charge ordering and type-*A* antiferromagnetism.

The development of the type-*A* AF phase correlates with a decrease in the resistivity of the material below T_{CO} and suggests that charge carriers in the AF phase become delocalized compared to the CO phase. Thus the coexistence here between the CO and AF phases also highlights the coexistence of two different electronic states. A similar picture has been proposed for the coexistence of a ferromagnetic metallic phase and a charge-ordered phase in $Pr_{0.7}Ca_{0.3}MnO_3$.[3,18] Indeed the photoinduced insulator-metal transition observed in that material is somewhat analogous to the transition from charge ordering to an antiferromagnetic insulator in $LaSr_2Mn_2O_7$. However, the *electronic phase separation* in $Pr_{0.7}Ca_{0.3}MnO_3$ is somewhat different from what we find in $LaSr_2Mn_2O_7$ in that the charge in both the CO and AF phases is essentially localized and in that the separation occurs between a charge-ordered state and an antiferromagnetic insulator.

We note here that although the orbital ordering we observe is consistent with the CE-antiferromagnetic structure, the observation of type-*A* antiferromagnetism is suggestive of a completely different orbital ordering as discussed by Mizokawa and Fujimori.[19] Type-*A* antiferromagnetism is consistent with charge ordering where the e_g charge resides in Mn^{3+} $d_{x^2-y^2}$ orbitals in the *ab* plane as opposed to $d_{3z^2r^2}$ as found in $LaSr_2Mn_2O_7$ and $La_{1/2}Ca_{1/2}MnO_3$. At any temperature we find no evidence of additional superlattice reflections with propagation vector $(\pm 1/2, \pm 1/2, 0)$ or $(e,0,1)$, which may indicate such an orbital ordering. Recently Takata *et al.*[20] have shown that in the type-*A* antiferromagnet $NdSr_2Mn_2O_7$, charge density measurements are consistent with charge residing in Mn $d_{x^2-y^2}$ orbitals in the *ab* plane, in the absence of any charge ordering, and a similar orbital ordering may occur in $LaSr_2Mn_2O_7$ at low temperatures.

IV. LATTICE INSTABILITIES IN $LaSr_2Mn_2O_7$

Raman scattering involves the inelastic scattering of light by electrons and thus provides a tool to probe not only the lattice vibrations of a system, but also variations in charge density.[21,22] The technique of resonant Raman scattering, where the light involved in the scattering process is resonant with a strong electronic transition or absorption edge is well known and has been extensively used in semiconductors and high-T_c materials.[23] In particular, if the energy of incident light is close to or in resonance with an electronic transition,

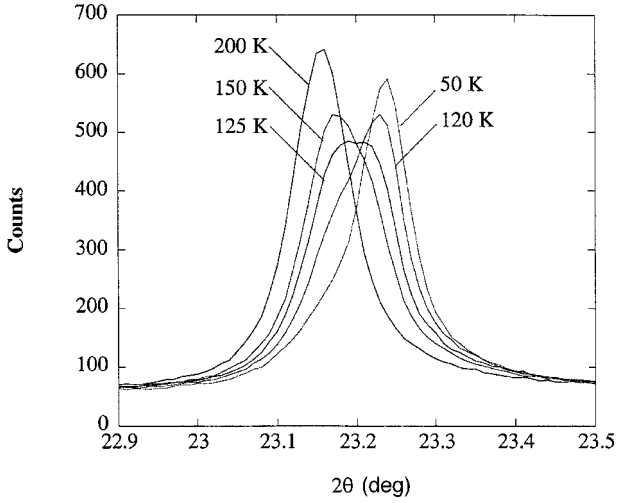

FIG. 3. The temperature dependence of the (0 0 10) peak profile measured using high-resolution x-ray diffraction.

a dramatic increase in the Raman intensity may be observed, as reported, for example, in $YBa_2Cu_3O_7$ and $La_{1.67}Sr_{0.33}NiO_4$.[24,25]

Raman scattering spectra were measured using three different energies (2.41, 2.54, and 2.7 eV), as a function of temperature from the powder sample of $LaSr_2Mn_2O_7$ (Fig. 4). The expected A_{1g} Mn-O lattice vibrations are observed at all excitation wavelengths (see Fig. 4), consistent with the single-crystal Raman measurements of $La_{1.2}Sr_{1.8}Mn_2O_7$ by Romero *et al.*[26] In particular, we observed the *in-plane* Mn-O(3) bending mode (δ_3) at 456 cm^{-1} and the *apical* Mn-O(2) stretching (ν_2) mode at 575 cm^{-1} (Ref. 26) at 300 K for all three excitation wavelengths [see Figs. 3(a) and 2 for labeling of atoms]. Moreover, the spectrum taken at 2.41 eV (514 nm) clearly shows two peaks that exhibit a resonant enhancement at approximately $490\,cm^{-1}(\delta_3')$ and $630\,cm^{-1}(\nu_2')$ at 300 K, as indicated by arrows in Fig. 4. Correlations among the intensity variations of these new resonant Raman modes as a function of temperature and frequency provide insight into the lattice instabilities near the CO and AF transitions. The resonant enhancement is consistent with a break in the symmetry of the electronic ground state of the system that gives rise to a resonance condition with an available excited *electronic* state in $LaSr_2Mn_2O_7$ as

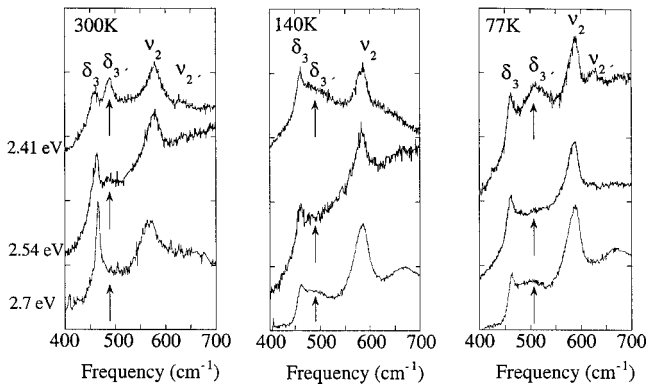

FIG. 4. Raman spectra measured at 300, 140, and 77 K using excitation wavelengths of 2.41, 2.54, and 2.7 eV.

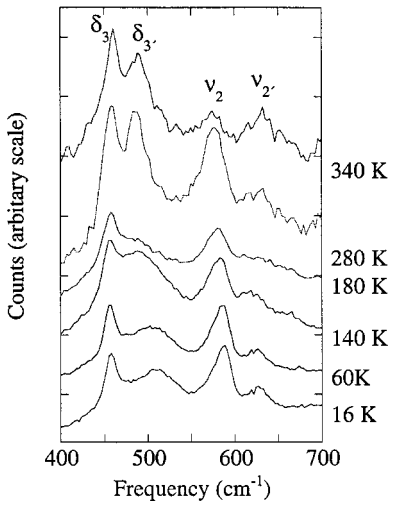

FIG. 5. Raman spectra as a function of temperature measured using an excitation wavelength of 2.41 eV.

has been observed in TTF-TCNQ and MX-linear chain complexes.[5]

In Fig. 5 we show the temperature-dependent resonant Raman spectra measured using an incident laser energy of 2.41 eV. These spectra reflect both the effects of the charge ordering, as seen in the resonant behavior and also the phase coexistence of the CO and AF phases as discussed in the previous section. As we shall show below, changes in the in-plane modes are sensitive to the charge ordering transition, while the apical modes are sensitive to the magnetic ordering and phase coexistence as discussed in the previous section. We shall deal with the two effects separately.

In-plane modes. The temperature dependence of the frequencies of the δ_3 and δ_3^- modes shows an anomalous behavior [see Fig. 6(a)]. The δ_3 mode softens by 3 cm^{-1} between 340 and 240 K, while both modes show an anomaly between 240 and 120 K where their frequency is constant as a function of temperature. Below 120 K, both modes return to a classical behavior and harden. The similarities of the frequencies of the δ_3 and δ_3' modes and their respective temperature dependences suggest that they are coupled and of the same percentage. In addition, the plateau in the temperature dependence of the frequency correlates with the observation of superlattice lines in the neutron and x-ray data and agrees with the symmetry of the δ_3 and δ_3' modes as they arise from in-plane vibrations. Similar resonant behavior has been observed in the charge-ordered nickelate $La_{1.67}Sr_{0.33}NiO_4$; resonant Raman modes appear at T_{CO} resulting from the different in-plane Ni-O bonds. Similarly, here the resonant Raman behavior of in-plane Mn-O(3) vibrations arises from the different bond lengths associated with the nominally $Mn^{3+}O_6$ and $Mn^{4+}O_6$ octahedra. Our observations differ compared to the $La_{1.67}Sr_{0.33}NiO_4$ compound in that the δ_3' mode is observed in the 2.41 eV spectra as high as 340 K, suggesting that critical charge fluctuations are present prior to the CO transition at 210 K. Associated with charge fluctuations, a Jahn-Teller coupling to phonon modes is expected, as the crystal structure would be modulated locally around hopping e_g charge carriers. With decreasing temperature our measurements suggest that charge-lattice fluctuations become static, in agreement with the observed symmetry lowering at T_{CO} and increase in resistivity as $T \rightarrow T_{CO}$. Furthermore, Raman intensity is also observed in the 2.54 and 2.7 eV spectra where the δ_3' mode is expected (see Fig. 3), which indicates a lowering of the crystallographic symmetry.

An overall increase in the intensity of the in-plane modes with decreasing temperature is also seen in Fig. 1(d), where the temperature dependence of the in-plane Mn-O(3) bending mode intensity has been integrated from 440 to 545 cm^{-1}. The integrated intensity is enhanced in the charge-ordered region and reflects a redistribution of the electronic spectra that tracks the resistivity of the material as well as the intensity of the observed superlattice reflections. We note here that although there is an overall enhancement in the integrated intensity of the in-plane Mn-O(3) modes, the temperature dependences of the widths of these modes are peculiar [see Fig. 6(a)]. The width of the δ_3 mode shows an

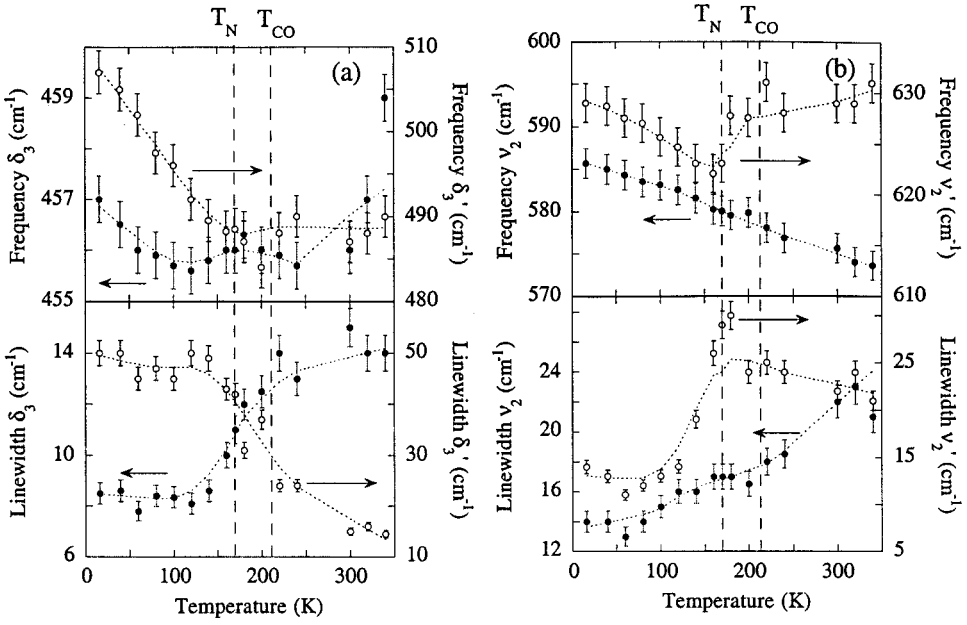

FIG. 6. Temperature dependence of the frequency and linewidths of (a) the δ_3 and δ_3' and (b) ν_2 and ν_2' Raman modes measured with an excitation wavelength of 2.41 eV.

abrupt decrease at T_{CO} consistent with the observed phase transition. However, the δ_3' mode shows the opposite behavior. Considering that the diffraction measurements clearly show a competition between the AF and CO phases, we suggest that this unusual broadening may mirror this competition: for example, the pinning of CO domains around point defects at low temperatures.

Apical modes. As with the in-plane Mn-O(3) modes, there is a smaller resonance effect associated with the Mn-O(2) apical modes ν_2 and ν_2'. From a structural perspective, variations in the charge density within the *ab* plane can result in different apical Mn-O bond lengths for nominally Mn^{3+} and Mn^{4+} ions. These changes appear to be small, as they were not detected in our diffraction measurements, but they are apparent in the Raman spectra. We observe a classical hardening of the ν_2 mode with decreasing temperature [see Fig. 6(b)]. The frequency of the ν_2' mode, on the other hand, decreases slowly with temperature until $\sim$180 K and then precipitously decreases at T_N. Below T_N, this mode exhibits a classical behavior. Furthermore, the width of this mode increases with decreasing temperature and then sharply decreases at $\sim T_N$, indicating a phase transition, while the width of the ν_2 mode shows a classical behavior [see Fig. 6(b)].

The changes in the Mn-O(2) stretching modes correlate with the development of the AF phase. As shown in the previous section, an unusual temperature dependence of the linewidth of the (0 0 10) reflection suggests that between T_{CO} and T^* there is a coexistence and competition between the CO and AF phases. These data further show a pronounced difference between the *c*-axis lattice parameters of these two phases consistent with the pronounced difference observed in the apical Mn-O(2) modes.

V. DISCUSSION

Charge-lattice fluctuations (electron-phonon coupling), which arise from dynamic hopping mechanisms such as polarons, are now generally accepted to play an important role in the charge transport properties of the manganite perovskites. Here Raman scattering provides an insightful picture for the region above T_{CO}. The resonant enhancement of modes coupled to *in-plane* vibrations suggests that dynamic charge-lattice fluctuations are present in $LaSr_2Mn_2O_7$ at temperatures as high as 340 K. Although we have not investigated the dispersion of these modes across the Brillouin zone, the observation of these fluctuations may be akin to dynamic charge ordering similar to what has been observed in $La_{1.85}Sr_{0.15}CuO_4$ by McQeeny *et al.*[1] What is clear from our Raman and diffraction measurements is that these charge-lattice fluctuations are a precursor to the CO transition at T_{CO}.

The strong electron-phonon coupling associated with the charge ordering transition in $La_{1/2}Ca_{1/2}MnO_3$ has recently been investigated using infrared spectroscopy and has been described in terms of a charge density wave.[27] These measurements show that a BCS-like gap $2\Delta(T)$ fully opens at low temperatures and follows the hysteretic ferromagnetic-antiferromagnetic transition. Currently, there are no such measurements for $LaSr_2Mn_2O_7$ to confirm whether the mechanism for the charge-ordering transition is the same as in $La_{1/2}Ca_{1/2}MnO_3$. The measurements presented in this paper do not probe similar anomalies in the infrared spectrum or on the Fermi surface. However, the observation of a coherent propagation vector and resonant Raman behavior are consistent with a charge-density-wave picture.

In broader terms, this work provides insight into the charge-lattice dynamics of the layered manganites. Dynamic and/or static charge-lattice fluctuations may be a typical feature of these materials. They appear to be stable above magnetic transitions in layered CMR manganites and melt with the development of in-plane ferromagnetic interactions, resulting in a reduction of the resistivity. The correlation length of these charge-lattice correlations may vary from long-range charge ordering as in $LaSr_2Mn_2O_7$ to shorter-range charge ordering correlations or polarons. Recent measurements by Vasiliu-Doloc *et al.*[28] have shown a somewhat similar behavior in the ferromagnetic-metallic-layered manganite $La_{1.2}Sr_{1.8}Mn_2O_7$. In this material charge correlations are observed at $\mathbf{q}=(h+\varepsilon,0,l=2n+1)$ above T_C and with coherence lengths of $\sim$20 Å, which melt close to the insulator-metal and ferromagnetic transitions.

VI. CONCLUSION

The observation of charge-lattice fluctuations above T_{CO}, an accurate description of the crystallographic structure of the CO phase, and the competition between CO and AF phases constitute an important step in the understanding of the charge-lattice dynamics in the layered manganite perovskites. From our measurements it is clear that charge-lattice fluctuations above T_{CO} become static with decreasing temperature and freeze to form a charge and orbitally ordered phase. This freezing is evident in both the observation of superlattice reflections and the increase in resistivity below T_{CO}. Our analysis of single-crystal neutron diffraction measurements shows that the charge and orbital ordering in $LaSr_2Mn_2O_7$ are similar to that found in the perovskite manganites and predicted by Goodenough. However, in stark contrast to the 3D perovskite manganites, the magnetic arrangement observed in the layered $LaSr_2Mn_2O_7$ is that of a type-*A* antiferromagnet, which is incompatible with the observed CE-type orbital ordering. This incompatibility is resolved in that charge ordering and type-*A* antiferromagnetism coexist as distinct and separate phases as shown by our x-ray diffraction measurements. The transition to type-*A* antiferromagnetism at lower temperatures is characterized by the competition between these two phases.

ACKNOWLEDGMENTS

The authors thank J. D. Jorgensen, H. Nakotte, M. S. Torikachvili, and J. M. Delgado for helpful discussions and comments on the manuscript. The work was supported by the U.S. Department of Energy, Basic Energy Sciences-Materials Sciences under Contract Nos. W-7405-ENG-36 (D.N.A., H.N.B., J.S.G.), and DE-AC02-98CH10886 (D.E.C.), and UCDRD Grant No. STB-UC:97-240 (H.N.B., G.F.S., K.H.) and by the MRL Program of the National Science Foundation under Award No. DMR96-32716 (B.J.C., A.K.C., A.D.S.).

*Present address: Materials Science Division, Argonne National Laboratory, Argonne, IL, 60439.
†Present address: Intense Pulsed Neutron Source, Argonne National Laboratory, Argonne, IL, 60439.
‡Present address: NPMR, Chalk River Laboratories, Bld. 459, Stn. 18, Chalk River, ON, KOJ 1JO, Canada.

[1] R. J. McQueeney, Y. Petrov, T. Egami, M. Yethiraj, G. Shirane, and Y. Endoh, Phys. Rev. Lett. **82**, 628 (1999).
[2] H. A. Mook and F. Dogan, Nature (London) **401**, 145 (1999).
[3] V. Kiryukhin, D. Casa, J. P. Hill, B. Keimer, A. Vigliante, Y. Tomioka, and Y. Tokura, Nature (London) **386**, 813 (1997).
[4] J. K. Furdyna and J. Kossut, *Diluted Magnetic Semiconductors* (Academic, New York, 1988).
[5] J. P. Pouget and R. Comes, in *Charge Density Waves in Solids*, edited by L. P. Gor'kov and G. Gruner (Elsevier, New York, 1989), p. 85.
[6] Y. Moritomo, A. Asamitsu, H. Kuwahara, and Y. Tokura, Nature (London) **380**, 141 (1996).
[7] D. N. Argyriou, J. F. Mitchell, P. G. Radaelli, H. N. Bordallo, D. E. Cox, M. Medarde, and J. D. Jorgensen, Phys. Rev. B **59**, 8695 (1999).
[8] T. G. Perring, G. Aeppli, T. Kimura, Y. Tokura, and M. A. Adams, Phys. Rev. B **58**, R14 693 (1998).
[9] T. Kimura, R. Kimai, Y. Tokura, J. Q. Li, and Y. Matsui, Phys. Rev. B **58**, 11 081 (1998).
[10] M. N. Iliev, M. V. Abrashev, H.-G. Lee, V. N. Popov, Y. Y. Sun, C. Thomsen, R. L. Meng, and C. W. Chu, Phys. Rev. B **57**, 2872 (1998).
[11] J. F. Mitchell, D. N. Argyriou, J. D. Jorgensen, D. G. Hinks, C. D. Potter, and S. D. Bader, Phys. Rev. B **55**, 63 (1997).
[12] P. G. Radaelli, D. E. Cox, M. Marezio, and S.-W. Cheong, Phys. Rev. B **55**, 3015 (1997).
[13] M. Kubota, H. Yoshizawa, Y. Moritomo, H. Fujioka, K. Hirota, and Y. Endoh, J. Phys. Soc. Jpn. **68**, 2202 (1999).
[14] D. N. Argyriou, T. Chatterji, and P. J. Brown (personal communication).
[15] J. B. Goodenough, Phys. Rev. **100**, 564 (1955).
[16] J. B. A. A. Elemans, B. V. Laar, K. R. v. d. Veen, and B. O. Loopstra, J. Solid State Chem. **3**, 238 (1971).
[17] P. D. Battle, D. E. Cox, M. A. Green, J. E. Milburn, L. E. Spring, P. G. Radaelli, M. J. Rosseinsky, and J. F. Vente, Chem. Mater. **9**, 1042 (1997).
[18] D. E. Cox, P. G. Radaelli, M. Marezio, and S.-W. Cheong, Phys. Rev. B **57**, 3305 (1998).
[19] T. Mizokawa and A. Fujimori, Phys. Rev. B **56**, R493 (1997).
[20] M. Takata, E. Nishbori, K. Kato, M. Sakata, and Y. Moritomo, J. Phys. Soc. Jpn. **68**, 2190 (1999).
[21] D. Steele, in *Theory of Vibrational Spectroscopy*, edited by R. Stevenson and M. A. Whitehead (Saunders, Philadelphia, 1971).
[22] D. K. Gardiner, in *Practical Raman Spectroscopy*, edited by D. K. Gardiner (Springer-Verlag, Berlin, 1989).
[23] M. Cardona, in *Light Scattering in Solids VI: Recent Results, Including High TC Superconductivity*, edited by M. Cardona and G. Guntherodt (Springer-Verlag, Berlin, 1991).
[24] G. Blumberg, M. V. Klein, and S.-W. Cheong, Phys. Rev. Lett. **80**, 564 (1998).
[25] E. T. Heyen, S. N. Rashkeev, I. I. Mazin, O. K. Andersen, R. Liu, M. Cardona, and O. Jepsen, Phys. Rev. Lett. **65**, 3048 (1990).
[26] D. B. Romero, V. B. Podobedov, A. Weber, J. P. Rice, J. F. Mitchell, R. P. Sharma, and H. D. Drew, Phys. Rev. B **58**, R14 737 (1998).
[27] P. Calvani, G. D. Marzi, P. Dore, S. Lupi, P. Maselli, F. D'Amore, and S. Gagliardi, Phys. Rev. Lett. **81**, 4504 (1998).
[28] L. Vasiliu-Doloc, S. Rosenkranz, R. Osborn, S. K. Sinha, J. W. Lynn, J. Mesot, O. H. Seeck, G. Preosti, A. J. Fedro, and J. F. Mitchell, Phys. Rev. Lett. **83**, 4393 (1999).